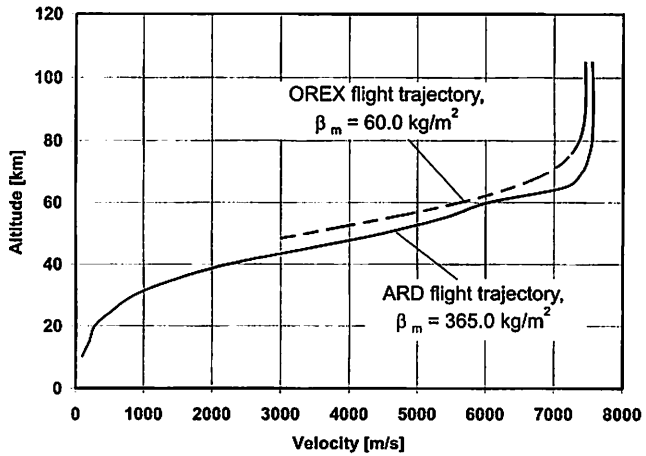

Fig. 5.2. Flight trajectories of OREX [8] and ARD [9].

ground conditions. It was launched in 1997 as a passenger on-board the American Mariner-Mark II CASSINI orbiter. After a flight of roughly seven years HUYGENS conducted a very successful entry into the Titan atmosphere in January 2005.

To ensure a stable ballistic flight and to master the thermal loads during entry in a not well-known atmosphere was the aerothermodynamic challenge of this mission. The composition of Titan's atmosphere consists approximately of 87 per cent N_2, 10 per cent Ar and 3 per cent CH_4 (in molar fractions).

Table 5.1. Ballistic factor $\beta_m = m/(A_{ref}C_D)$ of ballistic probes and lifting capsules.

Vehicle	Mass [kg]	A_{ref} [m^2]	Drag C_D	Ballistic factor β_m [kg/m^2]	Ref.
OREX	761.0	9.08	$\approx 1.40^{\alpha=0°}_{M=\infty}$	60.0	[10, 11]
EDV No.3	42.9	0.7854	$0.9595^{\alpha=0°}_{M=\infty}$	57.0	[12]
HUYGENS	$\approx$ 300.0	5.73	$\approx 1.52^{\alpha=0°}_{M=\infty}$	34.0	[13]–[15]
BEAGLE2	60.0	0.636	$\approx 1.45^{\alpha=0°}_{M=\infty}$	65.0	[16, 17]
ARD	2,800.0	6.16	$1.247^{\alpha=-22.8°}_{M=10}$	365.0	[18]
APOLLO	5,470.0	12.02	$1.247^{\alpha=-22.7°}_{M=10}$	365.0	[19, 20]
VIKING type	9,200.0	15.20	$1.391^{\alpha=-23.9°}_{M=10}$	435.0	[21]

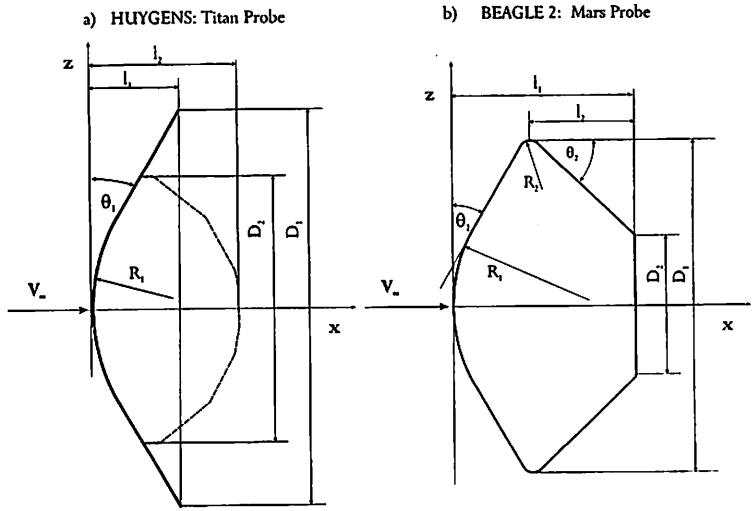

Fig. 5.3. Shape definition of the ballistic probes HUYGENS, [14, 15], and BEAGLE2, [16, 17]. HUYGENS has a rugged back contour which is idealized with a dashed line in the figure.

Table 5.2. Geometrical data and mission information of ballistic capsules.

Vehicle	Mission	v_e [km/s]	l_1 [mm]	l_2 [mm]	D_1 [mm]	D_2 [mm]	R_1 [mm]	R_2 [mm]	θ_1 [°]	θ_2 [°]
HUYGENS [14, 15]	Titan	6.0	620.5	985.0	2,700.0	1,790.0	1,250.0		30	
BEAGLE2 [16, 17]	Mars	5.63	499.5	212.0	900.0	371.8	417.0	29.0	30	43.75
OREX [10, 11]	Earth LEO	7.4	1,060.0		3,400.0	1,735.0	1,350.0	100.0	40	40

The geometrical definition of the HUYGENS probe is given in Fig. 5.3 a) and Table 5.2.

In the frame of a recent space mission to the planet Mars, the British small and low-cost probe BEAGLE2 was ejected from ESA's "Mars Express" (launched in June 2003) in order to conduct a ballistic entry into the Martian atmosphere. The capsule had a mass of 60 kg with a payload of 30 kg. Once having arrived at the Martian surface, a six-month scientific mission was planned to follow. The Martian atmosphere consists essentially of 97 per cent CO_2, 3 per cent N_2 (in molar fractions) and a trace amount of Ar. Besides the

provision of a reliable aerodynamic data base for a safe landing on the surface, the determination of the thermal loads was the main task of the planned mission [16, 17]. Unfortunately, BEAGLE2 was lost without knowing the exact reasons. Figure 5.3 b) shows the shape of BEAGLE2.

The space program in Japan had the objective of developing an unmanned winged orbiter called HOPE. To reach this goal, several demonstrators were designed and developed for getting aerodynamic and aerothermal data (and data for other disciplines like flight mechanics and vehicle control) in real free-flight environments. The Orbital Re-entry Experiment OREX was one of these demonstrators. It had a successful flight in Earth orbit and a subsequent ballistic re-entry in February 1994. The main tasks of this flight were to test the reliability of the TPS system (which was that one developed for HOPE) and to collect data of the hypersonic and supersonic aerodynamic and aerothermal behavior. We give, without further discussion, the data of OREX in Table 5.2 and Fig. 5.4.

5.2.2 Lifting Capsules

Capsules flying with an $L/D > 0$ while entering an atmosphere are called lifting capsules. If they have an axisymmetric shape, their angle of attack necessarily must be negative in order to achieve positive lift, Section 5.3. Mission information about such RV-NW's, the American APOLLO and the Russian SOYUZ vehicle being the most prominent ones, is given in Table 5.3.

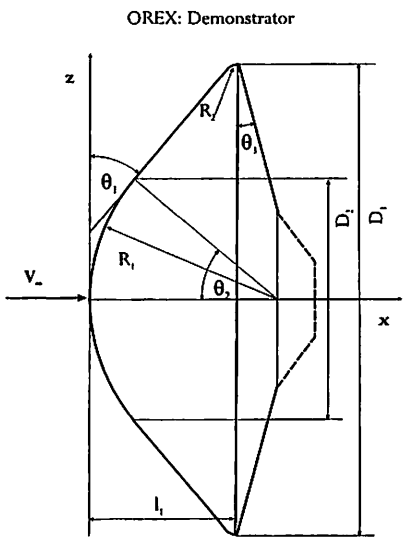

Fig. 5.4. Shape definition of the ballistic probe OREX, [10, 11].

There is no doubt that the aerothermodynamics of the APOLLO capsule are one of the best known. Due to the large number of flights in the 1960s and 1970s either in Earth orbit or of Lunar return, the free-flight data base is remarkable. During the design phase of APOLLO, most of the aerothermodynamic data was obtained from ground simulation facility experiments, [19, 20, 22, 28]–[30]. Heat transfer measurements in the hypersonic flow regime were conducted in "cold" hypersonic tunnels.

Some thirty years later in Europe, the Atmospheric Re-entry Demonstrator (ARD) was developed. Its shape was a sub-scaled APOLLO configuration with a modified rear part. In a first iteration, the aerodynamic data base for ARD was taken from APOLLO and later on improved. The advent of powerful numerical simulation methods had made it possible to strongly increase the understanding of complicated flow fields with multiple interactions of shocks, vortices and boundary layers, either attached or separated, with the influence of hot gases in thermodynamic equilibrium or non-equilibrium, with finite-rate catalytic wall conditions, and so on. Also new high-enthalpy facilities were available in Europe with the HEG in Germany and the F4 tunnel in France. These new capabilities were employed during the ARD's development phase. ARD was successfully flown in October 1998 and was recovered in the Pacific Ocean [18, 23, 31]. In Fig. 5.5 the shapes of APOLLO and ARD are plotted, while the corresponding geometrical values are listed in Table 5.4.

The Russian lifting capsule SOYUZ was the space transportation system to the Russian space station MIR. Since year 2001, besides the US Space Shuttle System, SOYUZ is guaranteeing the access to the International Space Station (ISS). Further, it acts as a rescue vehicle for the Space Station crew in case of any injury or sickness of the crew members [24].

Table 5.3. Mission information of lifting capsules.

Vehicle	Mission	V_e [km/s]	Ref.
APOLLO	Earth LEO	7.67	[20, 22]
	Lunar return	10.76	
ARD	Earth LEO	7.4	[18, 23]
SOYUZ	Earth LEO	7.9	[24]
VIKING 1	Earth LEO	7.9	[25]
AFE	Earth GEO	10.36	[4]
	Mars entry	5.70	
CARINA	Earth LEO	7.6	[26, 27]

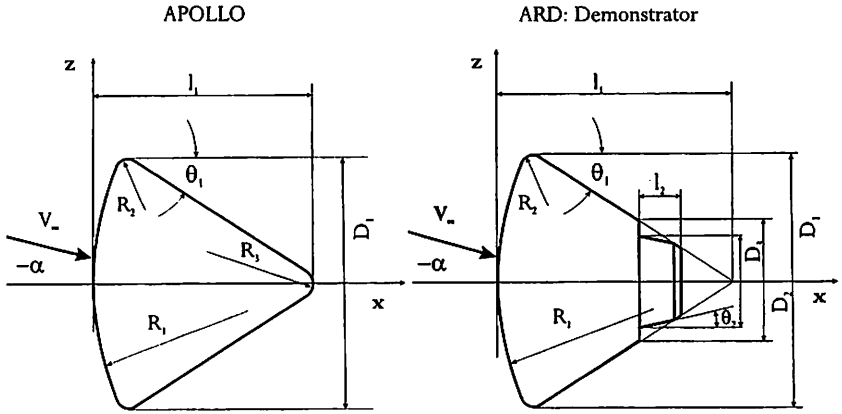

Fig. 5.5. Shape definitions of the lifting capsules APOLLO [20, 22] and ARD, [18, 23].

VIKING-type shapes are interesting configurations if non-winged solutions are sought for the transport of humans to and from space. In the frame of ESA's post-HERMES Manned Space Transportation Programme (MSTP) and the Crew Transport Vehicle (CTV) activities, VIKING-type shapes were investigated in very large detail by wind tunnel experiments, approximate engineering methods and highly sophisticated numerical simulation methods, Fig. 5.6.

Since the beginning of the space era, discussions about the advantage of aeroassisted orbital transfer vehicles have taken place. To realize this technique requires a very good knowledge of the aerodynamic and aerothermal behavior of the vehicle with respect to performance and controllability as well as thermal

Table 5.4. Geometrical data of lifting capsules, Figs. 5.5 to 5.7.

Vehicle	l_1 [mm]	l_2 [mm]	l_3 [mm]	D_1 [mm]	D_2 [mm]	D_3 [mm]	R_1 [mm]	R_2 [mm]	R_3 [mm]	θ_1 [°]	θ_2 [°]
APOLLO	3,529.0			3,912.0			4,694.0	196.0	232.	33	
ARD	2,594.0	460.0		2,800.0	1,317.0	1,015.	3,360.0	140.0		33	12
SOYUZ	2,142.0	1,778.	936.	2,200.0	980.0		2,235.0	978.0		11	7
VIKING 1	3,740.0			4,400.0			2,200.0	88.0		80	25
AFE	376.0			4,267.0						30	17
CARINA	1,263.0	482.0		1,078.0	634.0		4,380.0	2,124.0		13	

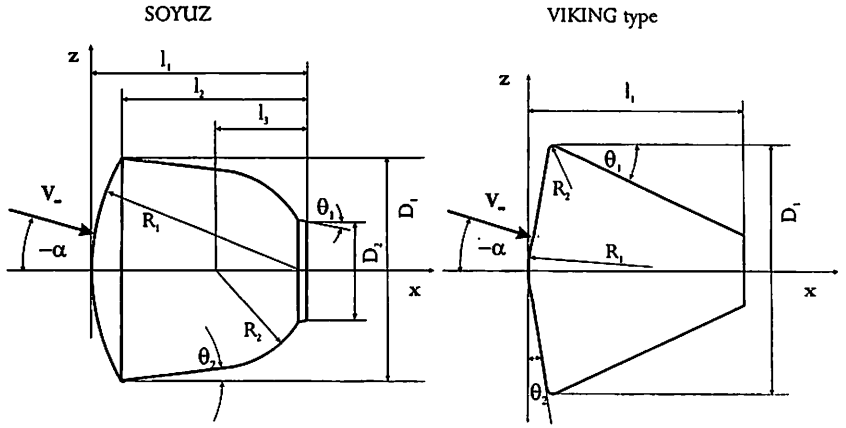

Fig. 5.6. Shape definitions of lifting capsules SOYUZ [24] and VIKING type [25].

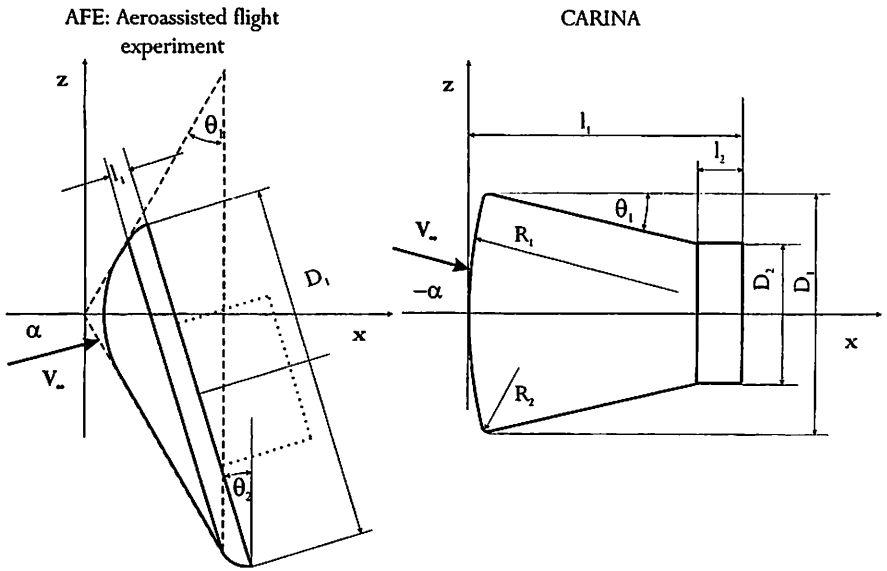

Fig. 5.7. Shape definitions of lifting capsules AFE [3, 32, 33], and CARINA [26].

loads. As was already mentioned, in order to improve the existing data bases in this regard, NASA had started in the 1980s a project with a generic configuration called Aeroassisted Flight Experiment (AFE), Fig. 5.7. Due to the asymmetric shape of AFE, the aerodynamic performance with $0.25 \lessapprox L/D \lessapprox 0.3$ is reached for a trim angle of attack $\alpha_{trim} \approx 0°$ with respect to the x-coordinate.

The expected advantages of this shape are twofold. First, an impingement

likely for moderate angle of attack variations or it happens farther downstream of the base compared to axisymmetric bodies. Secondly, the heating at the shoulders of the front shield, often the peak heating regime, is lower for AFE ($\alpha_{trim} \approx 0°$) due to the larger radii at the shoulders than for axisymmetric shapes with trim angles $\alpha_{trim} \approx -20°$.

The main goal of the aeroassisted orbital transfer technique is to reduce the relative orbital speed with the help of the atmosphere if for example an orbit transfer (from geostationary to low Earth orbit) or an atmospheric re-entry with supercritical speed (Lunar return) has to be conducted. The advantage of this process, today called aerocapturing, Sub-Section 5.1.2, is the possibility to dramatically decrease (up to 50 per cent) the total orbiter mass. This is mainly due to the fact that no (or a reduced) chemical propulsion system including the propellant, is needed compared to conventional missions.

Since the beginning of this century, there is a renewed interest in this technique in the frame of Mars exploration activities, where a Mars Sample Return Orbiter (MSRO) which has an AFE-like shape was generically defined and investigated in detail. The realization of this project (later than the year 2013 according to ESA's exploration plan) would be the first aerocapturing mission ever performed [3, 34].

In the 1990s, the Italian Space Agency (ASI) supported a satellite project named Capsula di Rientro Non Abitata (CARINA) for performing microgravity experiments in space. This system has the capability for atmospheric re-entry. The re-entry module of this system had a configuration based on the APOLLO/GEMINI shape and should have been able to return a payload mass of about 130 kg, Fig. 5.7 (right). An aerodynamic data base was established for the transonic through hypersonic Mach number range [26, 27].

5.2.3 Bicones

Since a long time, various bicones, fat (bluff) bicones, slender bicones, bent bicones, Fig. 5.8, were considered for particular space missions and some preliminary studies have been made. The advantage of these configurations is the higher lift-to-drag ratio L/D compared to simple capsules. Fat bicones have a $L/D \approx 0.6$, slender ones a $L/D \approx 0.9$ and bent bicones with even higher values of up to $L/D \approx 1.4$.[2] In contrast to the classical axisymmetric RV-NW's, these shapes achieve lift with a positive angle of attack. (Orbital transfer operations, where only the altitude of the orbit is changed, may be feasible with vehicles with a $L/D \approx 0.3$, but for missions with a change of the inclination of the target orbit, higher aerodynamic performance is necessary during the aerocapturing phase.) In general, bicones are appropriate for missions where a large cross-range capability, good maneuverability, low landing distortion (vehicle recovery), low entry loads are required, and for high entry velocities and thin atmospheres (low deceleration).

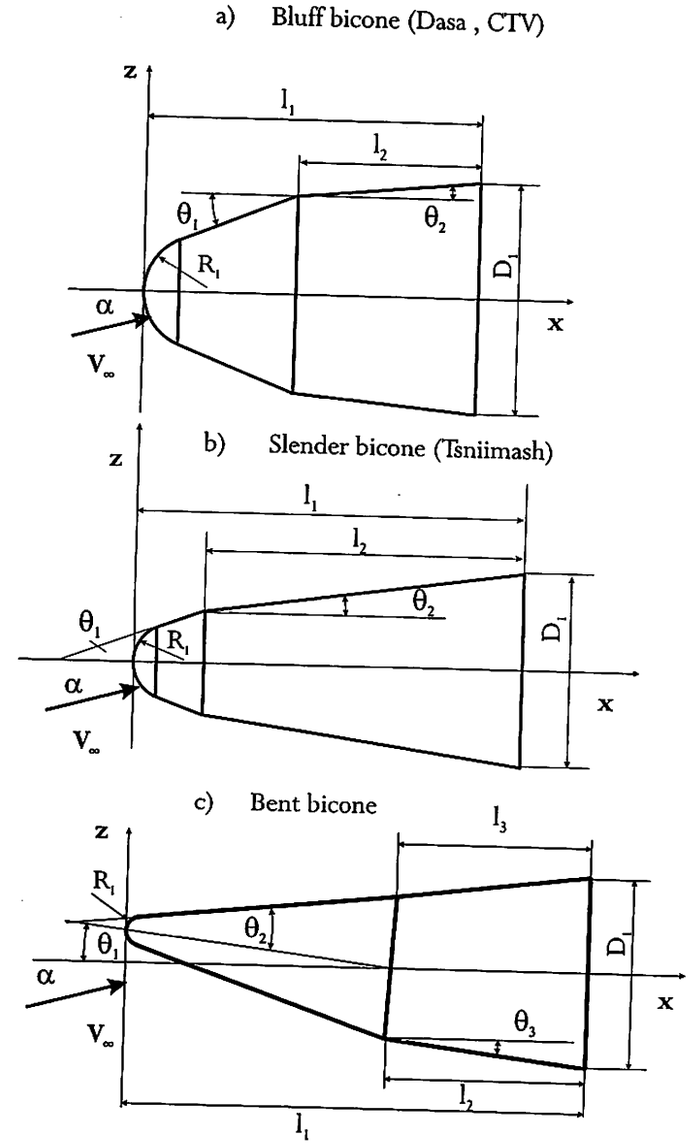

Fig. 5.8. Shape definitions of a) fat (bluff) bicone [36], b) slender bicone [24], and c) bent bicone [37].

Table 5.5. Geometrical data and mission information of bicones.

Vehicle	Mission	v_e [km/s]	l_1 [mm]	l_2 [mm]	l_3 [mm]	D_1 [mm]	R_1 [mm	θ_1 [°]	θ_2 [°]	θ_3 [°]
CTV DASA [36]	Earth LEO	7.6	6,300.0	3,425.0		4,400.0	1,056.0	22	5.4	
CTV ESA [24]	Earth LEO	7.6	6,830.0	3,745.0		4,398.0	882.0	20	7	
Slender Bicone [24]	Earth LEO	7.6	8,395.0	6,863.0		4,159.0	796.0	20	8	
Bent Bicone[3] [35], [37]	Earth LEO	7.6	182.52	80.85	77.32	76.20	5.79	7	12.84	7

Up to now none of these vehicles have reached a development state for performing a free flight (neither orbital nor suborbital). Some American reports inform about investigations in this field [35, 37]. In Europe several activities were performed in the frame of ESA's Crew Transport Vehicle (CTV) studies, [1, 36]. Also in Russia, there are some preliminary studies on biconic shapes [24]. Three of these biconic shapes can be found in Fig. 5.8 and the geometrical parameters are listed in Table 5.5.

5.3 Trim Conditions and Static Stability of RV-NW's

In this Section, we discuss the aerodynamic capabilities and potentials of various non-winged vehicles. For this, it is necessary to define the coordinate systems applied including those for the aerodynamic forces and moments, and to show what trim conditions and static stability mean. General formulas and definitions describing the aerodynamic state of all kind of vehicles are found in Chapter 7.

5.3.1 Park's Formula

For capsule-like shapes at supersonic and hypersonic Mach numbers and different angles of attack, it is observed that the line of action of the resultant aerodynamic force crosses the axis of symmetry (namely the x-coordinate) approximately at the same position. This intersection point is called the metacenter x_{cp}, Fig. 5.9. In cases where the aerodynamic coefficients are known for a few discrete angles of attack, this observation can be helpful for determining the

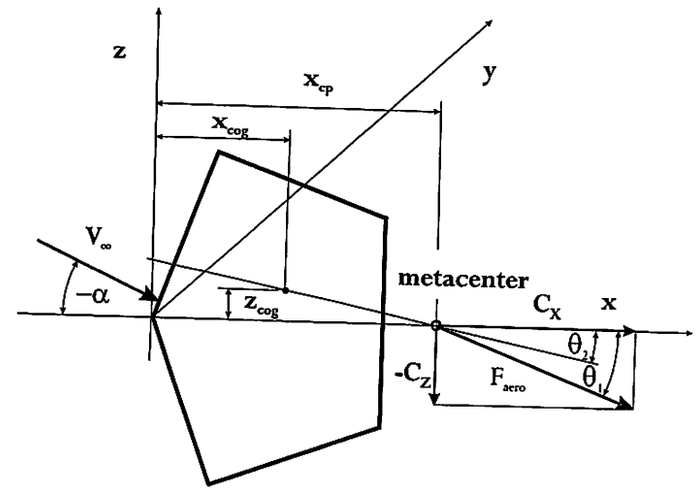

Fig. 5.9. Definition of the metacenter.

trim angle of attack. This is often the situation, if the aerodynamic data are obtained with the help of numerical simulation methods, where non-equilibrium thermodynamics, catalytic walls, turbulent flow, etc., are taken into account, which makes the computations (still) very expensive and time consuming.

We assume that x_{cp} and the force coefficients C_X and C_Z are nearly independent of α (for $M_\infty \gtrapprox 2$) and $\partial C_m/\partial\alpha$ is approximately constant.[4] With eq. (7.2), we can write

$$L_{ref} C_m(\alpha_j)|_{cog} - C_Z(\alpha_j)(x_{cog} - x_{cp}) + C_X(\alpha_j) z_{cog} = 0, \qquad z_{cp} = 0, \quad (5.2)$$

$$C_m(\alpha_{trim})|_{cog} = 0, \quad (5.3)$$

$$C_m(\alpha_j)|_{cog} + (\alpha_{trim} - \alpha_j)\frac{\partial C_m(\alpha_j)}{\partial\alpha} = 0, \quad (5.4)$$

$$-\left\{\frac{L_{ref}\alpha_j}{C_Z(x_{cog} - x_{cp})}\frac{\partial C_m(\alpha_j)}{\partial\alpha}\left(\frac{\alpha_{trim}}{\alpha_j} - 1\right) + 1\right\}\frac{C_Z(\alpha_j)}{C_X(\alpha_j)} + \frac{z_{cog}}{x_{cog} - x_{cp}} = 0. \quad (5.5)$$

In these equations α_{trim} denotes the trim angle of attack and α_j the angle of attack, where the aerodynamic coefficients are known. Further we obtain from eq. (7.14):

$$-L_{ref}\alpha_j\frac{\partial C_m(\alpha_j)}{\partial\alpha} = -\alpha_j\frac{\partial C_Z(\alpha_j)}{\partial\alpha}(x_{cog} - x_{cp}) + \alpha_j\frac{\partial C_X(\alpha_j)}{\partial\alpha} z_{cog}. \quad (5.6)$$

[4] This holds, for instance, for the VIKING 2 shape, Fig. 5.10, and also some others